

DPSK PERFORMANCE OF A NAKAGAMI FADED DS/SSMA SYSTEM WITH DIVERSITY

Pieter van Rooyen * and Fritz Solms †

* Department of Electrical and Electronic Engineering, University of Pretoria, Pretoria, 0002

† Department of Applied Mathematics, RAU, P.O. Box 524, Johannesburg 2006

Abstract. This work considers the performance of Direct Sequence Spread Spectrum Multiple Access (DS/SSMA) transmission with space- and time diversity for the uplink of a cellular Indoor Wireless Communication (IWC) channel. Due to fading associated with the IWC channel and the asynchronous arrival of the received signals a coherent reference is difficult to obtain and hence Differential Phase Shift Keying (DPSK) is assumed as modulation scheme. The indoor communication channel, which is multipath faded, is modeled by a discrete set of Nakagami faded paths which has been shown to fit empirical data of the IWC channel better than other distributions [1]. Instead of using the commonly assumed Gaussian Assumption to describe the Inter User Interference (IUI), the Maximum Entropy (MaxEnt) method [2] is used to infer the IUI distribution accurately [3]. The average error rate and capacity of a DS/SSMA system under typical IWC channel conditions is therefore accurately calculated using the IUI distribution obtained by the MaxEnt method. Numerical results reveal that for non-diversity receivers, Nakagami fading is very hostile to the SSMA signal. However, using space diversity with Maximum Ratio Combining (MRC) and time diversity (in the form of convolutional coding) at the base station, the average error rate can be reduced dramatically, allowing for reliable communication.

Key Words. Spread Spectrum, Error Control Coding

1. Introduction

Spread spectrum signaling techniques, with its inherent anti-multipath, multiple access and rejection of interference capabilities have increasingly received attention for cellular personal and mobile communications. Until recently the standard analysis of SSMA systems was rather pessimistic about the capacity of these systems compared to FDMA and TDMA. Gilhousen et al [4] recognized that since SSMA capacity is only interference limited (unlike FDMA and TDMA) any reduction in interference converts directly and linearly into an increase in capacity. Therefore, by employing a voice activity factor, sectorizing the cells and using various forms of diversity it is possible to achieve SSMA system capacity at least as good as FDMA and TDMA. This improvement has been indicated by [4] and others under AWGN conditions.

In this paper a detailed analysis of the performance of a cellular SSMA system with diversity under frequency selective slowly fading Nakagami and multipath conditions is presented. For the channel to be frequency selective, the bandwidth of the transmitted signal should exceed the coherence bandwidth of the channel [5]. The coherence bandwidth is related to the mean delay spread of the channel which is typically 60-100 ns [6] for the IWC channel. For diversity purposes, space

diversity with MRC and time diversity, realized by convolutional error correcting coding, are considered to be present at the base station.

There is a sizable literature relating to the effects of multiple access interference on the performance of cellular DS/SSMA, among which are [7] and [8]. Most literature, except Xiang [7], assume either Rayleigh or Rician fading statistics to model the IWC channel. It has been shown, however, that the Nakagami distribution assumes the signals are received with random moduli and phases, leading to more flexibility in matching experimental data than that of Rayleigh or Rice models, i.e. [9] and [10] to mention a few. This is especially true for the indoor wireless and densely built urban channels. A mathematical analysis have been performed by Nakagami [11] and more recently by Braun et al [12] to derive the Nakagami distribution and it has been shown to be a fundamental physical model. For a detailed discussion of the Nakagami distribution as a model for fading [5] and [13] can be consulted.

Normally the IUI distribution (due to the non-ideal correlation properties of the spreading codes) of a DS/SSMA system is assumed to be Gaussian distributed [14]. This assumption has been shown to be inaccurate under certain conditions [15]. In this paper we make use of the MaxEnt principle to determine the actual IUI distri-

bution by calculating the moments of the IUI variable. However, for comparative purposes, closed form expressions are derived when the IUI distribution are assumed to be Gaussian distributed. Therefore, using the equations derived in this work it is possible to predict DS/SSMA capacity under the mentioned conditions with space- and time diversity. By introducing a voice activity factor of 3/8 and cell splitting of 3, the performance of a cellular system is assessed. It is assumed that hard decisions are made by the MRC demodulator and that these hard decisions are fed to the convolutional decoder. It is further assumed that the error-producing mechanism results in independent error events. The latter assumption requires interleaving at the transmitter and de-interleaving at the receiver. Section 2 analyses and describes a system model for a typical Nakagami fading channel. The analyses allows for the calculation of the average error probabilities by means of closed form expressions, making use of the Gaussian Assumption to model the multiple access interference. A discussion of the diversity techniques and numerical results are discussed in Sections 3 and 4 respectively. Finally, conclusions are presented in the last section of the paper. The appendices give an expression for the IUI moments and the necessary background to the MaxEnt method.

2. System model and evaluation

The model considered will be summarized briefly and is based on the model developed by Kavehrad [8].

As mentioned earlier, the capacity of a DS/SSMA system is interference limited and therefore, reducing the interference, increases the system capacity. Measurements by Qualcomm [20] indicate that the adjacent cell interference in a cellular system contribute approximately 50% of the total interference (for equally loaded cells). Therefore, assuming equally loaded cells, the maximum number of users a cellular system can support is given by [21]

$$K' = K \frac{N_{sect}}{V_{on}} 1.5 \quad (1)$$

where K is the total number of users per cell, V_{on} the voice activity factor and N_{sect} the cell splitting factor. Our conjectural system will assume $\frac{N_{sect}}{V_{on}} = 8$.

The channel for the desired transmitter and receiver ($k = 1$) can be represented by an L -paths Nakagami fading model where a single transmitted pulse is received via L -paths at the random

instant $t_l, l = 1, \dots, L$. We assume t_l is uniformly distributed over one bit period $(0, T)$ and that each user code sequence has a period of $N = T/T_c$.

In the analysis we assume that average power control is assumed which also includes averaging the channel fading characteristics. Baseband signaling at a rate less than the channel coherence bandwidth ensures that intersymbol interference can be neglected. Therefore, the channel has a low-pass equivalent impulse response, given by

$$h(t) = \sum_{l=1}^L \beta_l \delta(t - t_l) e^{j\phi_l}, \quad (2)$$

where $\delta(\cdot)$ is the delta function, β_l is the Nakagami distributed path gain and ϕ_l is the random path phase, uniformly distributed between $(0, 2\pi]$.

In the transmission model it is further assumed that the k th interfering user of the multiple access system is linked to the receiver via a single Nakagami fading path with a uniformly distributed random delay τ_k ranging from zero to one bit period, T . This will naturally result in a worst case scenario, rendering the results conservative.

In our formulation we specify the Nakagami distributed path gain of the $K - 1$ interfering users by $V_k, k = 2, \dots, K$. Thus, the received signal for the fading model described is given by

$$\begin{aligned} r(t) = & A \sum_{l=1}^L \beta_l a_1(t - t_l) b_1(t - t_l). \quad (3) \\ & \cos(\omega_c t + \Phi_l) + A \sum_{k=2}^K V_k a_k(t - \tau_k) \\ & b_k(t - \tau_k) \cos(\omega_c t + \Psi_k) + n_c(t) \cos(\omega_c t) \\ & + n_s(t) \sin(\omega_c t) \end{aligned}$$

where $\Phi_l = \theta_1 - \omega_c t_l + \phi_l$, $\Psi_k = \theta_k - \omega_c \tau_k$ and θ_k the phase of the k th user. Also, $n(t)$ has been expressed in terms of its lowpass equivalent components $n_s(t)$ and $n_c(t)$ [22]. The carrier phase θ_k has been absorbed in the random phase ϕ_k associated with each channel path.

We arbitrarily choose user $k = 1$ as the reference user and calculate the probability of error of the data symbol b_0^1 . At time $t = T$, the nominal sampling point for matched filter detection, we have [23]

$$\begin{aligned} \zeta_c(T) = & A \sum_{l=1}^L \beta_l \left\{ b_{-1}^1 R_{1,1}(t_l) + b_0^1 \hat{R}_{1,1}(t_l) \right\} \cdot (4) \\ & \cos \phi_l + A \sum_{k=2}^K V_k \left\{ b_{-1}^k R_{k,1}(\tau_k) + b_0^k \hat{R}_{k,1}(\tau_k) \right\}. \end{aligned}$$

$$\cos \phi_k + \eta,$$

and

$$\begin{aligned} \zeta_s(T) = & A \sum_{l=1}^L \beta_l \sin \phi_l. \\ & \left\{ b_{-1}^1 R_{1,1}(t_l) + b_0^1 \hat{R}_{1,1}(t_l) \right\} \\ & + A \sum_{k=2}^K V_k \sin \phi_k. \\ & \left\{ b_{-1}^k R_{k,1}(\tau_k) + b_0^k \hat{R}_{k,1}(\tau_k) \right\} \\ & + \nu, \end{aligned} \quad (5)$$

with the definitions of b_0^k , b_{-1}^k , $R_k(\tau)$ and $\hat{R}_k(\tau)$ as defined in [14], and

$$\eta = \int_0^T a_1(s) n_c(s) ds, \quad (6)$$

and

$$\nu = \int_0^T a_1(s) n_s(s) ds. \quad (7)$$

The noise samples η and ν are independent zero-mean Gaussian random variables with equal variance $\sigma_n^2 = N_0 T$ [24]. Notice that the intersymbol interference here is due to partial correlation and involves only the previous bit. For most indoor channels, the delay spread is considerably less than the bit intervals of practical interest and the partial correlation intersymbol interference is the only type present.

Now, let us assume without loss of generality that $t_1 = 0$ and $\phi_1 = 0$. That is, we assume that the first path ($L = 1$) between the transmitter of user 1 and the corresponding receiver is the reference path and all other paths constitute interference. Let z_1 denote the complex envelope of the matched filter output at the sampling instant, i.e. $z_1 = \zeta_c(T) + j\zeta_s(T)$. Since the fading is slow compared to the data rate, we may assume that the corresponding complex envelope at the previous sampling instant, denoted z_2 , differs from z_1 only in the data bits involved and in the additive Gaussian noise samples. It is therefore easily shown that

$$z_1 = \beta_1 AT b_0^1 \quad (8)$$

$$\begin{aligned} & + AT \left\{ \sum_{l=2}^L \beta_l X_l \cos \phi_l + \sum_{k=2}^K V_k X_k \cos \phi_k \right\} \\ & + jAT \left\{ \sum_{l=2}^L \beta_l X_l \sin \phi_l + \sum_{k=2}^K V_k X_k \sin \phi_k \right\} \\ & + (\eta_1 + j\nu_1), \end{aligned}$$

and

$$\begin{aligned} z_2 = & \beta_1 AT b_{-1}^1 \\ & + AT \left\{ \sum_{l=2}^L \beta_l Y_l \cos \phi_l + \sum_{k=2}^K V_k Y_k \cos \phi_k \right\} \\ & + jAT \left\{ \sum_{l=2}^L \beta_l Y_l \sin \phi_l + \sum_{k=2}^K V_k Y_k \sin \phi_k \right\} \\ & + (\eta_2 + j\nu_2), \end{aligned} \quad (9)$$

with

$$\begin{aligned} X_l &= b_{-1}^1 R_{1,1}(t_l) + b_0^1 \hat{R}_{1,1}(t_l) \\ X_k &= b_{-1}^k R_{k,1}(\tau_k) + b_0^k \hat{R}_{k,1}(\tau_k) \\ Y_l &= b_{-2}^1 R_{1,1}(t_l) + b_{-1}^1 \hat{R}_{1,1}(t_l) \\ Y_k &= b_{-2}^k R_{k,1}(\tau_k) + b_{-1}^k \hat{R}_{k,1}(\tau_k). \end{aligned} \quad (10)$$

In (9), the data bit b_{-2}^k of the k th user is transmitted two-bit intervals prior to b_0^k . The noise variables η_1 , η_2 , ν_1 and ν_2 are independent of one another, and the binary data bits are equal to +1 or -1 with equal probability. The output of the DPSK demodulator at the sampling instant is given by

$$\zeta = \text{Re}[z_1 z_2^*], \quad (11)$$

where * denotes complex conjugate.

Let us indicate the transmitted DPSK signals as $s_1(t)$ and $s_2(t)$. In relation to the received signal, $z_1(t)$ and $z_2(t)$, the following binary signal pair is transmitted

$$\begin{aligned} s_1(t) &= (z_1(t), z_1(t)) \quad \text{or} \quad (z_2(t), z_2(t)) \\ s_2(t) &= (z_1(t), z_2(t)) \quad \text{or} \quad (z_2(t), z_1(t)) \end{aligned}$$

As explained before, the first T seconds of each

waveform are actually the last T seconds of the previous waveform. Note that $s_1(t)$ and $s_2(t)$ can each have either of two possible forms and that $z_1(t)$ and $z_2(t)$ are antipodal signals. Therefore, pairs of DPSK signals can be represented as orthogonal signals $2T$ long. Detection could correspond to non-coherent envelope detection with four channels matched to each of the possible envelope outputs. Since the two envelope detectors representing each symbol are negatives of each other, the envelope of each will be the same. Hence the detectors can be implemented as a single channel matched to $s_1(t)$ or $s_2(t)$.

The probability of error can now be calculated by realizing that

$$P_e = P(\zeta > s_2 | z_2). \quad (13)$$

where s_2 is used to indicate the random variable of $s_2(t)$.

Making the assumption that the variables $z_1(t)$ and $z_2(t)$ are Gaussian distributed the following analysis can be performed. (The validity of this assumption is investigated in Section 4.1 and should not be confused with the previously stated GA).

For the case where $z_2(t)$ is sent, the output of $z_1(t)$ will be only Gaussian noise, and therefore the output of the envelope detector is noise having a Rayleigh distribution, given by

$$p_{z_1|s_2} = \frac{z_1}{\sigma_n^2} \exp \left\{ -\frac{z_1^2}{2\sigma_n^2} \right\} \quad \forall z_1 \geq 0, \quad (14)$$

where σ_n^2 is the noise at the filter output.

On the other hand $z_2(t)$ has a Rice distribution since the input to the envelope detector is Gaussian noise plus a signal component. The pdf is written as

$$p(z_2|s_2) = \frac{z_2}{\sigma_n^2} \exp \left\{ -\frac{z_2^2 + m_2^2}{2\sigma_n^2} \right\} I_0 \left(\frac{z_2 m_2}{\sigma_n^2} \right) \quad (15)$$

with

$$m_2 = \frac{(\beta_1 + \alpha)AT}{2}, \quad (16)$$

which is the average of the Gaussian decision variable and α the multiple access random variable.

Now, when s_2 is transmitted, the receiver makes an error whenever the envelope sample $z_1(t)$ exceeds the envelope sample $z_2(t)$. Thus the probability of this error can be obtained by integrating $p(z_1|s_2)$ with respect to $z_1(t)$ from $z_2(t)$ to infinity, and then averaging over all possible values of $z_2(t)$. That is,

$$P_e = \int_0^\infty p(z_2|s_2) \left\{ \int_{z_2}^\infty p(z_1|s_2) dz_1 \right\} dz_2 \quad (17)$$

$$\int_0^\infty \frac{z_2}{\sigma_n^2} \exp \left\{ -\frac{z_2^2 + m_2^2}{2\sigma_n^2} \right\} I_0 \left(\frac{z_2 m_2}{\sigma_n^2} \right) \left\{ \int_{z_2}^\infty \frac{z_1}{\sigma_n^2} \exp \left\{ -\frac{z_1^2}{2\sigma_n^2} \right\} dz_1 \right\} dz_2.$$

Using integration tables by [25], the integral in (17) is evaluated analytically as

$$P_e = \frac{1}{2} \exp \left\{ -\frac{m_2^2}{2\sigma^2} \right\} \quad (18)$$

After substituting (16) in (17) we have an expression for the conditional error rate for DPSK signaling

$$P_{e|\beta_1, \alpha} = \frac{1}{2} \exp \left\{ -(\beta_1 + \alpha)^2 \frac{E_b}{N_0} \right\}. \quad (19)$$

The conditioning in α can be removed by the integration

$$P_{e|\beta_1} = \int_{-\infty}^\infty P_{e|\beta_1, \alpha} p(\alpha) d\alpha. \quad (20)$$

where $p(\alpha)$ is the distribution of the IUI.

2.1. Calculation of Error Probability using MaxEnt

At this point it is possible to determine (20) using either the MaxEnt principle, or making use of the Gaussian Approximation (GA), that is assuming the IUI distribution to be Gaussian distributed. The accuracy of the MaxEnt method relative to the GA will be showed in a later section.

Using the MaxEnt principle $p(\alpha)$ can be accu-

rately assessed and by using

$$\bar{\gamma}_b = E\{\beta_i^2\} \frac{E_b}{N_0}, \quad (21)$$

$$p(\gamma_b) = \left(\frac{m}{\gamma_b}\right)^\epsilon \frac{\gamma_b^{\epsilon-1}}{\Gamma(\epsilon)} \exp\left(-\frac{m\gamma_b}{\gamma_b}\right) \quad (22)$$

$$\forall \gamma_b \geq 0,$$

and $\epsilon = mP$ (m the Nakagami fading parameter and P the number of diversity branches) the conditioning in α and β_1 of (20) can be removed.

2.2. Calculation of Error Probability using the GA

One of the most popular approximations to the IUI is the GA, in which the overall multiple access interference is approximated by a Gaussian random variable. It is easy to apply and can be easily generalized to systems with more advanced modulation schemes, such as MPSK and QAM. The rationale behind the GA is that the overall IUI consists of the contributions from many different interferers and the IUI from each interferer consists of many contributions from many chips. In such situations, central limit arguments may apply and the overall IUI may be approximated by a Gaussian random variable. In this section the GA is used to derive the average probability of error.

In this case $p(\alpha)$ is assumed to be a zero mean Gaussian distribution with variance $\sigma_{ma}^2 = \frac{K-1}{3N}$. The result after integrating (20) is

$$P_{e|\beta_1} = \frac{1}{2} \exp\left(-\Lambda \beta_1^2 \frac{E_b}{N_0}\right) \quad (23)$$

with

$$\frac{1}{\Lambda} = 1 + 2 \frac{E_b}{N_0} \sigma_{ma}^2. \quad (24)$$

Using (21) and (22) the conditioning in β_1 of (23). The result after integration by parts is

$$P_e = \frac{1}{2} \left(1 + \frac{\gamma_0 \Lambda}{m}\right)^{-\epsilon}, \quad (25)$$

which is the result for DPSK SSMA signaling un-

der Nakagami fading.

Without multiple access interference and $m = 1$, (25) reduces to

$$P_e = \frac{1}{2} \left\{ \frac{1}{1 + \gamma_0} \right\} \quad (26)$$

which is the well known performance of a single-path Rayleigh fading channel, i.e. [5].

As $m \rightarrow \infty$ and $P = 1$, that is no fading, and using the identity [25]

$$\lim_{m \rightarrow \infty} \left(1 + \frac{z}{m}\right)^{-m} = \exp(-z) \quad (27)$$

it is easily shown that

$$\lim_{m \rightarrow \infty} \frac{1}{2} \left(1 + \frac{\gamma_0 \Lambda}{m}\right)^{-\epsilon} \quad (28)$$

$$= \frac{1}{2} \exp\left\{ \left(\frac{N_0}{E_b} + 2\sigma_{ma}^2 \right)^{-\frac{1}{2}} \right\},$$

which is similar to an expression derived at under non-fading conditions [15].

3. Diversity Techniques

In this section an overview of the two diversity techniques to enhance the system performance are discussed. Diversity techniques are based on the notion that errors occur in reception when the channel attenuation is large, i.e. when the channel is in a deep fade. If we can supply to the receiver several replicas of the same information signal transmitted over independently fading channels, the probability that all the signal components will fade simultaneously is reduced considerably. There are several ways in which we can provide the receiver with independent fading replicas of the same information bearing signal. In this paper it is assumed that space diversity is provided by a number of antennas at the base station. It is also assumed that an additional form of diversity are provided by error control coding in the time domain, that is by supplying the same information signal spread over a number of redundant bits.

The two diversity schemes, that is space- and time diversity work together in the following fashion. After the antennas at the base station receive the faded signals, they are combined in an optimal

way called Maximum Ratio Combining [5]. Hard decisions are made after the combining process and then passed on to the convolutional decoder where error correction is performed.

The following two sections describe respectively the combining process used after space diversity and the bounds used to calculate the error control coding gain.

3.1. Maximum Ratio Combining

After the independently faded signals are received by the base station the signals are combined to form an estimate of the transmitted signal. The combiner that achieves the best performance is one in which each matched filter output is multiplied by the corresponding complex-valued channel gain. The effect of this multiplication is to compensate for the phase shift in the channel and to weight the signal by a factor that is proportional to the signal strength. Thus, a strong signal carries a larger weight than a weak signal. After the complex-valued weighting operation is performed, two sums are formed. One consists of the real parts of the weighted outputs from the matched filters corresponding to a transmitted 0. The second consists of the real part of the outputs from the matched filters corresponding to a transmitted 1. The optimum combiner is called a Maximum Ratio Combiner (MRC) [5]. Of course the realization of this optimum combiner is based on the assumption that the channel attenuations and the phase shifts are known perfectly. That is, the estimates of the parameters contain no noise. Only the ideal case (no noise) condition is investigated in this paper.

3.2. Error Control Coding

Error control coding can be used with great success in SSMA with no penalty paid in bandwidth by the addition of redundancy to the information bits. It is further shown that low rate coding can be used very efficiently in a SSMA system. In this work rate $R_{cd} = \{\frac{1}{2}, \frac{1}{4}, \frac{1}{8}\}$ constrained length $\nu = \{2, 3, 4\}$ convolutional codes are considered.

It is assumed that the PN spreading sequence spans one code symbol. This implies that under the assumption of fixed throughput (i.e. constant data rate), fixed maximum chip rate and fixed complexity, a rate R_{cd} code must employ a PN spreading sequence shorter by a factor R_{cd} than that of the uncoded case. This results in increased inter user interference due to the poorer cross correlation properties of shorter PN sequences. In our case we use PN sequences of $N = 511$ for the uncoded case and $N = 255, 127$ and 63 for rate

$R_{cd} = \{\frac{1}{2}, \frac{1}{4}, \frac{1}{8}\}$ codes respectively.

As explained in [5, 26, 27], when considering maximum likelihood decoding (Viterbi decoding) with hard decision decoding, the probability of selecting an incorrect path in the decoder trellis, can be represented by

$$P_2(d) = \sum_{k=(d+1)/2}^d \binom{d}{k} P_e^k (1 - P_e)^{d-k} \quad (29)$$

$\forall \quad d \text{ odd}$

and

$$P_2(d) = \sum_{k=d/2+1}^d \binom{d}{k} P_e^k (1 - P_e)^{d-k} \quad (30)$$

$$+ \frac{1}{2} \binom{d}{d/2} P_e^{d/2} (1 - P_e)^{d/2}$$

$\forall \quad d \text{ even.}$

The first event error probability can be bounded by the sum of the error probabilities $P_2(d)$ over all possible paths which merge with the all zero path at the given node. In (29) and (30) P_e is the probability of error obtained from (19). We therefore obtain the union bound

$$P_u < \sum_{d=d_{free}}^{\infty} a_d P_2(d), \quad (31)$$

where the coefficients $\{a_d\}$ represent the number of paths corresponding to the set of distances $\{d\}$. These coefficients are the coefficients in the expansion of the transfer function $T(D)$ [5]. The coefficients of $\{a_d\}$ were obtained from [5] and [13].

The sum of (31) is approximated by a finite number of terms since it converges very quickly. Even under fading conditions, with the assumption of interleaving, a finite number of terms are sufficient to obtain accurate results.

4. Numerical Results

In the subsequent evaluations, with no loss of generality, the normalization $\Omega = -10$ dB is adopted so that the received energy in the fading channel, $\beta_1^2 E_b$, has an average value $E\{\beta_1^2 E_b\} = \Omega E_b = 0.1 E_b$. With $\Omega = 0.1$, the Nakagami pdf is reduced to a one-parameter distribution so that all

the results can be expressed in terms of the single parameter m . To investigate the influence of the Nakagami parameter m , five values are investigated; $m = \{\frac{1}{2}, 1, 2, 3, 5\}$. For $m = 1$ the Nakagami pdf reduces to the Rayleigh pdf and hence can be used for benchmark purposes. The parameter m is inversely proportional to the amount of fading. In other words, as m increases the pdf tends to an impulse response and consequently represents no fading.

4.1. Comparison between MaxEnt and the GA

To investigate the accuracy of the GA and the assumption made earlier in Section 2, let us examine Figure 1. We note that, as with most Gaussian approximations, that the GA results in less conservative performance results. As m grows, it is seen that the GA becomes less valid, which is also the case when no diversity is present. As P increases, the GA becomes less valid.

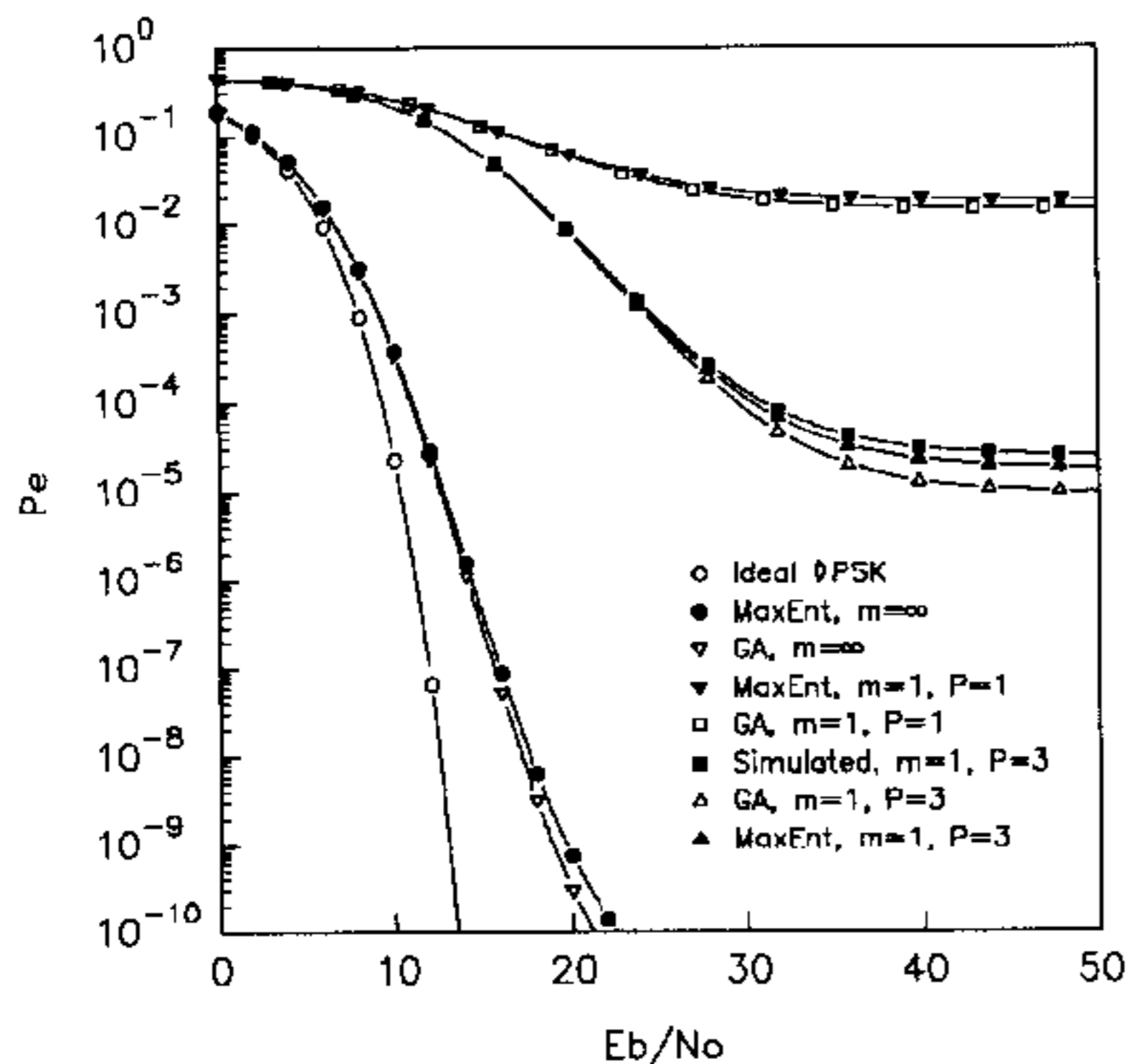


Fig. 1. Accuracy of the GA with DPSK signaling: $m = \{\infty, 1\}$, $K = 30$, $N = 511$ and $P = \{1, 3\}$

Also included in Figure 1 is a computer simulation for $P = 3$ to quantify the GA and the assumption of Section 2. It is clear that the MaxEnt result is closer to the simulated curve than the GA result. By making the assumption as described in Section 2 our results are slightly inaccurate but within acceptable limits.

Results obtained with the GA is less valid since, by examining the decision statistics carefully, it can be seen that the contributions from different interferers are, in general, dependent, and the contributions from different chips of the same interferer are also dependent. Hence the widely used Central Limit Theorem (CLT) for independent

random variables does not apply. The exact conditions for the overall IUI to converge to a Gaussian random variable are not clear. In fact, to the best of our knowledge, there is no proof that the overall IUI converges to a Gaussian random variable under any conditions. It is therefore necessary to use more exact approximations of the IUI. One of the most accurate methods is to use the MaxEnt method and it has been applied with great success lately [28, 29, 3].

4.2. Nakagami Performance without Diversity

Figure 2 indicates the performance for $K = 2$ and $L = 1$. It is apparent that the average error rate decreases substantially as m increases. For $m = \frac{1}{2}$, severest fading, the performance for as little as two users is very poor and saturates at an error rate of 10^{-2} and consequently the system fails as a multiple access system for $m < 1$.

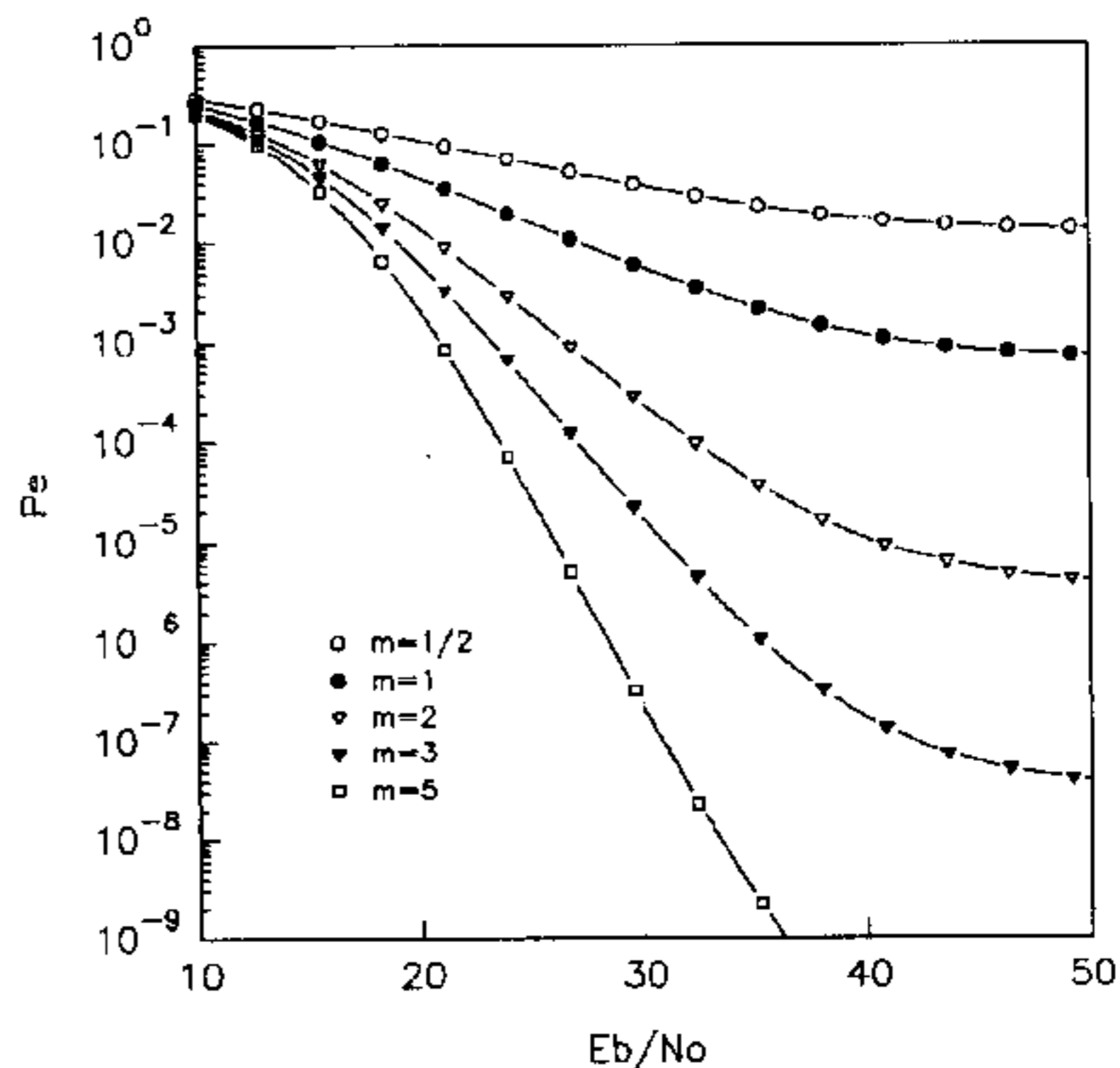


Fig. 2. Nakagami faded DPSK performance: $K = 2$, $L = 1$ and $N = 511$

Table 1 indicates the capacity of a Nakagami faded SSMA system for different values of m and L at $E_b/N_0 = 60$ dB. The case $m = \infty$ represents the unfaded performance and also the value that the capacity of a Nakagami faded channel will saturate at.

Using Table 1 and (25) it is possible to calculate the capacity of a cellular system with voice activity monitoring and cell splitting. It is clear that by virtue of a cellular architecture it is possible to increase the system capacity by a factor of eight. However, the capacity of such a system is still relatively low and it is clear that some form of diversity is needed to substantially increase the system capacity, especially under multipath fading conditions.

	P_e	$L = 1$	$L = 5$	$L = 10$
$m = 1/2$	10^{-3}	-	-	-
$m = 1$	10^{-3}	2	-	-
$m = 2$	10^{-3}	18	13	7
	10^{-5}	2	-	-
$m = 3$	10^{-3}	37	32	26
	10^{-5}	8	2	-
$m = 5$	10^{-3}	62	57	50
	10^{-5}	20	15	8
	10^{-8}	5	-	-
$m = \infty$	10^{-3}	115	-	-
	10^{-5}	63	-	-
	10^{-8}	36	-	-

Table 1 K for non-diversity DPSK: $E_b/N_0 = 60$ dB, $P = 1$ and $L = \{1, 5, 10\}$

4.3. Nakagami Performance with MRC Diversity

Figure 3 indicates the performance improvement by using a MRC receiver for $L = 3$ and a three branch ($P = 3$) diversity receiver for $K = 30$. For $m = \frac{1}{2}$ and a three tap MRC receiver the average error rate is decreased substantially, ensuring at least $K = 30$ at an error rate of 10^{-3} .

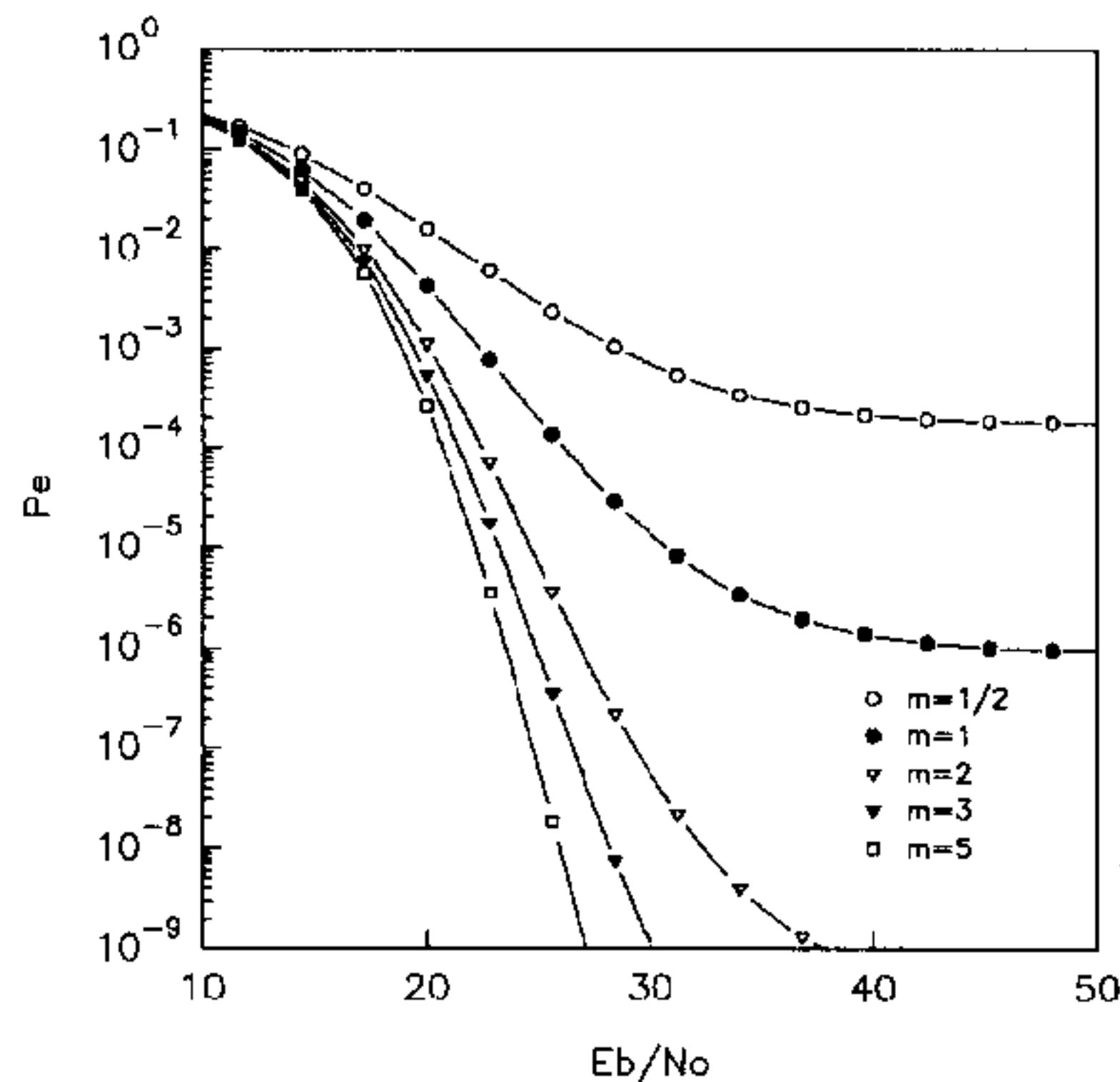


Fig. 3. Nakagami faded DPSK performance: $K = 30$, $L = 3$, $P = 3$, $N = 511$ and $m = \{\frac{1}{2}, 1, 2, 3, 5\}$

As benchmark, the performance for $m = 1$ is also indicated in Figure 3. Again the performance is substantially improved as the number of taps, P , increases. For a three tap MRC receiver with $m = 1$, the performance is approximately three orders better than for the $m = \frac{1}{2}$ case.

Figure 4 indicates the capacity, K , as a function of P for different values of m . We therefore note that the capacity saturates to less than a 1000 users as P increases.

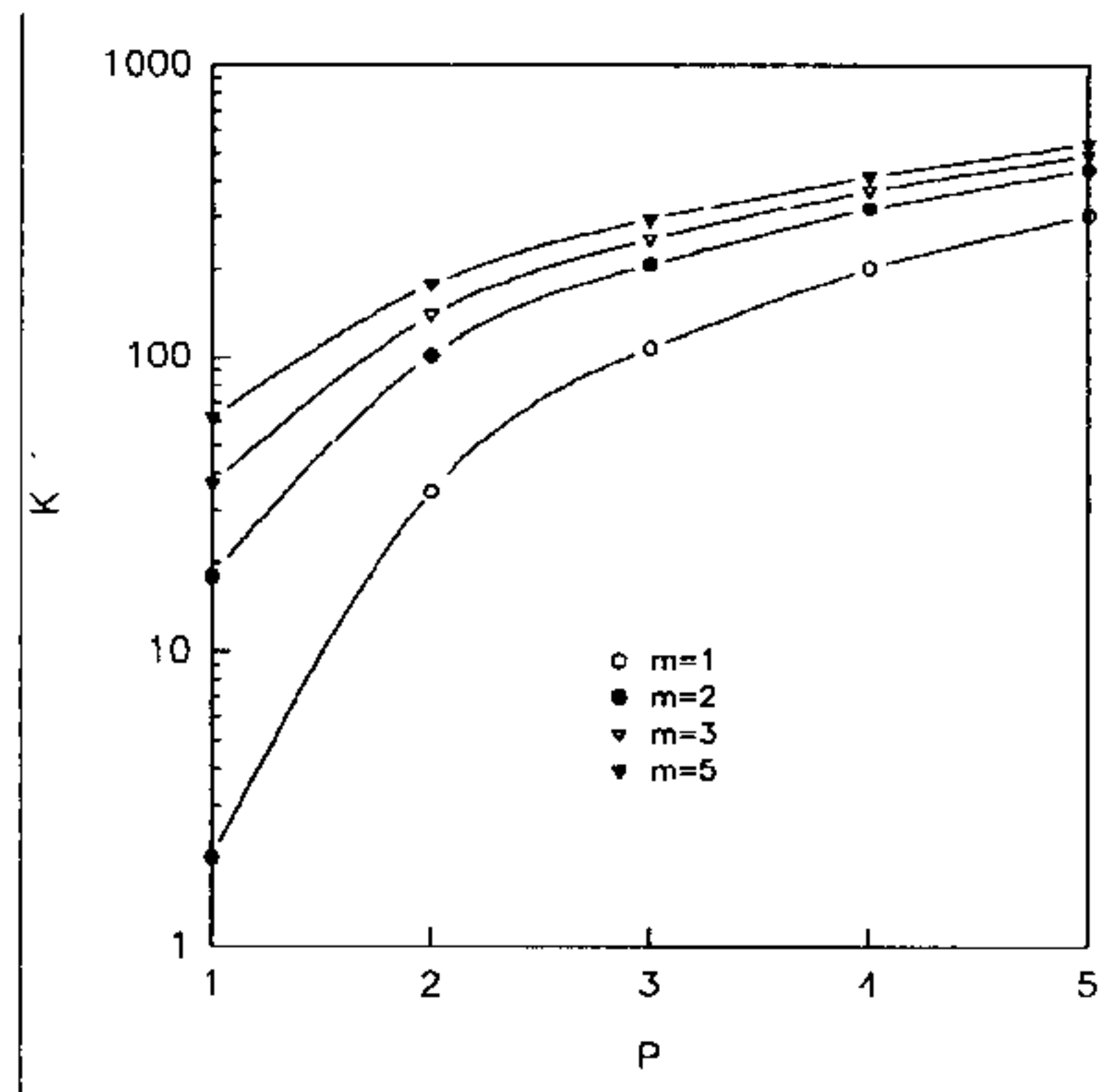


Fig. 4. Capacity of a P branch system

	P_e	$P = 2$	$P = 3$	$P = 4$	$P = 5$
$m = 1/2$	10^{-3}	2	3	68	134
	10^{-5}	-	-	3	16
$m = 1$	10^{-3}	35	108	202	305
	10^{-5}	3	19	51	94
	10^{-8}	-	-	6	18
$m = 2$	10^{-3}	102	208	322	439
	10^{-5}	27	73	130	191
	10^{-8}	4	19	43	73
$m = 3$	10^{-3}	139	254	372	492
	10^{-5}	49	75	171	236
	10^{-8}	13	39	72	108
$m = 5$	10^{-3}	177	296	416	537
	10^{-5}	78	142	210	277
	10^{-8}	30	65	104	143

Table 2 K for MRC diversity DPSK: $E_b/N_0 = 60$ dB, $P = \{2, 3, 4, 5\}$ and $L = \{2, 3, 4, 5\}$

Table 2 indicates the capacity of a single cell Nakagami faded system with MRC diversity up to five branches. A linear increase in K with P is noticeable. As before, the cellular capacity can be obtained by multiplying the indicated values by a factor of five when voice activity and sectorization are included.

4.4. Nakagami Performance with Convolutional Coding

As another form of diversity, we consider the performance of a SSMA system under Nakagami fading with convolutional coding. As mentioned before, coding can be implemented very efficiently in a spread spectrum system. Table 3 indicates the capacity improvement due to rate $R_{cd} = \{\frac{1}{2}, \frac{1}{4}, \frac{1}{8}\}$

convolutional codes with constrained length $\nu = 4$.

	P_e	$\nu = 2$	$\nu = 3$	$\nu = 4$
$m = 1/2$	10^{-3}	4	11	35
	10^{-5}	-	2	16
	10^{-8}	-	-	6
$m = 1$	10^{-3}	28	28	61
	10^{-5}	9	14	36
	10^{-8}	2	6	19
$m = 2$	10^{-3}	68	44	78
	10^{-5}	35	27	52
	10^{-8}	14	15	33
$m = 3$	10^{-3}	89	58	85
	10^{-5}	52	33	58
	10^{-8}	26	20	38
$m = 5$	10^{-3}	110	56	90
	10^{-5}	71	38	63
	10^{-8}	40	25	43
$m = \infty$	10^{-3}	135	122	98
	10^{-5}	94	85	69
	10^{-8}	62	57	48

Table 3 K for convolutional coded DPSK at $E_b/N_0 = 60$ dB, $P = 1$, $L = 1$, $R_{cd} = \frac{1}{8}$ and $N = 63$

It is interesting to note that low rate coding becomes effective as m increases. In other words if the channel is highly faded, i.e. $m = \frac{1}{2}$, low rate convolutional coding can be used to increase system capacity. However, as $m = \infty$, that is no fading, half rate coding is the most effective.

4.5. Nakagami Performance with MRC Diversity and Coding

It is shown that low rate convolutional coding is not very effective when m is small. Therefore, Table 4 indicates only the performance of half rate convolutional codes combined with a P branch diversity receiver. The performance is greatly enhanced by a combination of coding and diversity. The improvement over the uncoded, non-diversity case is 909% at $m = 5$, $P = 5$ and $P_e = 10^{-3}$.

From this table it is clear that a combination of convolutional coding and MRC diversity is very effective in enhancing the capacity. Moreover, combining error control codes and diversity is bandwidth and power efficient since the average error rate saturates at lower values of E_b/N_0 .

5. Conclusions

In this paper the MaxEnt technique was used to accurately calculate the performance of a DS/SSMA system. It has been shown that this

	P_e	$P = 2$	$P = 3$	$P = 4$	$P = 5$
$m = 1/2$	10^{-3}	54	150	267	395
	10^{-5}	17	66	136	217
	10^{-8}	2	18	51	94
$m = 1$	10^{-3}	135	265	401	541
	10^{-5}	69	153	247	344
	10^{-8}	26	74	131	194
$m = 2$	10^{-3}	202	342	484	628
	10^{-5}	124	223	323	425
	10^{-8}	67	131	198	267
$m = 3$	10^{-3}	229	371	515	658
	10^{-5}	149	250	352	455
	10^{-8}	88	156	225	296
$m = 5$	10^{-3}	252	396	540	684
	10^{-5}	171	274	377	480
	10^{-8}	108	178	249	320

Table 4 K for convolutional coded and MRC diversity DPSK, $R_{cd} = \frac{1}{2}$, $\nu = 4$ and $N = 255$

technique delivers more accurate results than the Gaussian Assumption.

From the numerical results it is apparent that Nakagami fading with small values of m is very hostile to a SSMA signal. Small values of m correspond to the more general Rayleigh fading channel ($m = 1$) and more severe fading than Rayleigh fading ($m < 1$). As m increases, the results indicate that the performance gets more acceptable. Using diversity, specifically MRC combining reception and convolutional coding, it is possible to increase the capacity of a Nakagami faded SSMA signal substantially. Only hard decision decoding was considered, but it is assumed that soft decision decoding will further improve the system performance.

Convolutional coding is probably a simpler means to obtain diversity, but has the drawback that interleaving is required. Especially in a speech based system interleaving can lead to excessive and unacceptable delays. MRC combining reception on the other hand is more complex, but with advances in ASIC technology, this problem can be surmounted in the near future.

The results presented can be applied to a typical rural environment in an informal settlement area. The communication channel in these settlements is typical of a Nakagami fading environment since it is similar to a build up urban area or IWC channel environment.

To conclude, to guarantee acceptable performance under Nakagami fading conditions some form or forms of diversity is absolutely necessary - the type of diversity needed is to be dictated by the

specific application and cost considerations.

6. Appendix A

This section briefly states an expression for the moments used as input to the MaxEnt method. For a detailed derivation of these moments [3] can be consulted.

The IUI distribution, α is a function of the independent random parameters τ_k, Θ_k and b_1^k . Furthermore, α is symmetrically distributed and hence the odd moments of α_k are all zero. Therefore, having the even moments one can determine the moments as

$$N_m = \frac{\binom{2j}{j}}{4^j} \frac{E\{V_k^{2j}\}}{N^{2j+1}} \sum_{n=0}^{N-1} \sum_{r=0}^j \binom{2j}{2r} \Gamma_{j,r,n} \quad (32)$$

with $\Gamma_{j,r,n}, A_{n_{k,1}}, B_{n_{k,1}}, \hat{A}_{n_{k,1}}$ and $\hat{B}_{n_{k,1}}$ as defined in [13].

Further, we notice that for a Nakagami distribution

$$E\{V_k^{2j}\} = \frac{\Gamma(\epsilon + j)}{\Gamma(\epsilon)} \left(\frac{\nu_{0k}}{m}\right)^j 2^j, \quad (33)$$

where $\nu_{0k} = E\{V_k^2/2\}$ is the average strength of the Nakagami faded path associated with the k th interfering user.

7. Appendix B

In this section the MaxEnt method is summarized. For a detailed discussion of the MaxEnt principle [13, 3] can be consulted.

In the MaxEnt method the missing information (the information entropy) [16]

$$I = - \int_a^b p(\alpha) \ln p(\alpha) d\alpha \quad (34)$$

is maximized subject to the constraints of the normalization of the pdf and subject to the available information. In our case the expectation values of the moment operators must be equal to the measured or calculated moments. This is a standard maximum entropy moments problem which has been studied in great detail [17, 18]). The constraints are introduced via Lagrange multipliers and the resulting expression for the inferred pdf

is

$$p(\alpha) = \frac{1}{Z} \exp\left(-\sum_{m=1}^M \lambda_m \alpha^m\right) \quad (35)$$

where the information about the normalization is contained in the partition function

$$Z = \int_a^b \exp\left(-\sum_{m=1}^M \lambda_m \alpha^m\right) d\alpha \quad (36)$$

and the Lagrange multipliers are determined by requiring that

$$\langle \alpha^m \rangle \equiv \int \alpha^m p(\alpha) d\alpha = \mu_m \quad ; \quad m = 1, \dots, M \quad (37)$$

where the μ_m are the known moments of the IUI random variable.

From (35) a closed form expression of the IUI distribution is available and it can be used to calculate the average error rate. All the information contained in the available moments (and no more) are used to determine the IUI distribution.

Alhassid et al. [19] have noted that defining

$$F(\{\lambda_m\}) = \ln Z + \sum_{m=1}^M \lambda_m \mu_m \quad (38)$$

yields

$$\frac{\partial F}{\partial \lambda_m} = \mu_m - \langle \alpha^m \rangle \quad (39)$$

Hence minimizing F is equivalent to solving the set of coupled nonlinear equations (37). Furthermore, the authors have shown that the Hessian matrix \mathbf{H} with

$$H_{mm'} = \frac{\partial^2 F}{\partial \lambda_m \partial \lambda_{m'}} = \langle \alpha^{m+m'} \rangle - \langle \alpha^m \rangle \langle \alpha^{m'} \rangle \quad (40)$$

is positive definite and thus that F is a strictly convex function of the Lagrange multipliers $\{\lambda_m\}$. Consequently F has a unique minimum (i.e. (37) has a unique solution) and a Newton-Raphson minimization procedure [18] is guaranteed to converge. Define an error vector

$$\bar{\epsilon} = (\epsilon_1, \dots, \epsilon_M)^T \quad ; \quad \epsilon_m \equiv \mu_m - \langle \alpha^m \rangle \quad (41)$$

and let $\bar{\lambda} = (\lambda_1, \dots, \lambda_M)$. Then the new guess after a Newton Raphson step is

$$\bar{\lambda}' = \bar{\lambda} - \mathbf{H}^{-1} \cdot \bar{\epsilon} \quad (42)$$

During each iteration we solve a set of coupled linear equations for the Newton step $\bar{\delta} = \bar{\lambda} - \bar{\lambda}'$

$$\mathbf{H} \cdot \bar{\delta} = \bar{\epsilon} \quad (43)$$

Since \mathbf{H} is positive definite it is also non-singular. We solve equation (43) with a standard LU-decomposition with a back-substitution algorithm coded in C^{++} .

REFERENCES

- [1] U. Charash, "Reception through Nakagami fading multipath channels with random delays," *IEEE Transactions on Communications*, vol. COM-27, pp. 657-670, April 1979.
- [2] J. E. Shore and R. W. Johnson, "Axiomatic derivation of the principle of Maximum Entropy and the principle of Minimum Cross-Entropy," *IEEE Transactions on Information Theory*, vol. IT-26, no. 26, pp. 26-37, 1980.
- [3] F. Solms, P. van Rooyen, and J. Kunicki, "Maximum entropy and minimum relative entropy in performance evaluation of digital communication systems," *IEE Proceedings-I*, no. 5, pp. 12-15, 1995.
- [4] K. Gilhousen, I. Jacobs, R. Padovani, and L. Weaver, "Increased capacity using CDMA for mobile satellite communications," *IEEE Transactions on Selected Areas in Communication*, vol. 8, pp. 503-514, May 1990.
- [5] J. Proakis, *Digital Communications*. McGraw-Hill, New York - third edition, 1995.
- [6] M. Kavehrad and P. McLane, "Performance of Low-complexity Channel Coding and Diversity for Spread Spectrum in Indoor Wireless Communication," *AT&T Technical Journal*, vol. 64, pp. 1927-1965, October 1985.
- [7] H. Xiang, "Binary Code-Division Multiple-Access Systems operating in Multiple Fading, Noisy channels," *IEEE Transactions on Communications*, vol. COM-33, no. 8, pp. 775-784, August 1985.
- [8] M. Kavehrad, "Performance of Nondiversity Receivers for spread spectrum in Indoor Wireless Communications," *AT&T Technical Journal*, vol. 64, no. 6, pp. 1181-1210, July-August 1985.
- [9] M. A. Mokhtar and C. Gupta, "Power control considerations for DS/CDMA personal communication systems," *IEEE Transactions on Vehicular Technology*, vol. 41, pp. 479-487, November 1992.
- [10] P. Crepeau, "Uncoded and coded performance of MFSK and DPSK in Nakagami fading channels," *IEEE Transactions on Communications*, vol. 40, pp. 487-493, March 1992.
- [11] M. Nakagami, *The m-distribution - A general formula of intensity distribution of rapid fading*. Elmsford, NY: Pergamon, 1960.
- [12] W. R. Braun and U. Dersch, "A Physical Mobile radio Channel Model," *IEEE Transactions on Vehicular Technology*, vol. 40, pp. 472-482, May 1991.
- [13] P. van Rooyen, *Maximum Entropy based analysis of a DS/SSMA diversity system*. PhD thesis, Rand Afrikaans University, Johannesburg, November 1994.
- [14] M. Pursley, "Performance Evaluation for Phase-Coded SSMA Communications - Part 1: System Analysis," *IEEE Transactions on Communications*, vol. COM-25, no. 8, pp. 795-803, August 1977.
- [15] G. L. Turin, "The Effects of Multipath and Fading on the Performance of Direct-Sequence CDMA Systems," *IEEE Journal on Selected Areas in Communications*, vol. SAC-2, pp. 597-603, July 1984.
- [16] C. E. Shannon, "A mathematical theory of communications," *Bell systems technical journal*, no. 27, p. 379, 1948.
- [17] A. Tagliani, "On the application of Maximum Entropy to the moments problem," *Journal on Mathematical Physics*, no. 34, pp. 326-337, 1993.
- [18] L. Mead and N. Papanicolaou, "Maximum Entropy in the Problem of Moments," *Journal on Mathematical Physics*, vol. 25, pp. 2404-2417, August 1984.
- [19] N. Agmon, Y. Alhassid, and R. Levine, "An upper bound for the entropy and its application to the maximal entropy problem," *Journal on Computational Physics*, no. 30, p. 250, 1979.
- [20] "An overview of the application of CDMA to digital cellular systems and personal cellular networks," tech. rep., Qualcomm Inc., San Diego, Ca, May 1992.
- [21] P. van Rooyen, "CPSK Performance of a Micro Diversity DS/SSMA System," *Transactions of the South African Institute of Electrical and Electronic Engineers*, vol. 86, pp. 65-72, June 1995.
- [22] L. Couch, *Digital and analog communication systems*. Macmillan Publishing Co., 1983.
- [23] M. Kavehrad and B. Ramamurthi, "Direct sequence spread spectrum with DPSK modulation and diversity for indoor wireless communications," *IEEE Transactions on Communications*, vol. COM-35, pp. 224-236, February 1987.
- [24] B. Sklar, *Digital communications: Fundamentals and Applications*. Prentice Hall, 1988.
- [25] M. Abramowitz and I. Stegman, *Handbook of Mathematical functions*. Washington, D.C.: National Bureau of Standards, 1964.
- [26] G. C. Clark and J. Cain, *Error-Correcting Coding for Digital Communications*. Plenum Press, 1981.
- [27] S. Lin and D. Costello, *Error Control Cod-*

- ing: Fundamentals and Applications*. Prentice Hall, 1983.
- [28] P. van Rooyen, F. Solms, and R. Kohno, "Maximum Entropy Investigation to the distribution of the Inter User Interference of a DS/SSMA system," *IEEE Transactions on Communications*, submitted for publication.
- [29] P. van Rooyen, J. Kunicki, and R. Pichna, "Performance of cellular SSMA with block coding under fading and multipath conditions," in *Proceedings of ISSSTA '94*, (Oulu, Finland), pp. 263–267, July 1994.